Proc. Natl. Acad. Sci. USA
Vol. 93, pp. 8123–8128, July 1996
Plant Biology

Changes in voltage activation, Cs^+ sensitivity, and ion permeability in H5 mutants of the plant K^+ channel KAT1

DIRK BECKER*, INGO DREYER*, STEFAN HOTH*, JOHN D. REID†, HEINER BUSCH*, MICHAELA LEHNEN‡, KLAUS PALME‡, AND RAINER HEDRICH*§

*Institut für Biophysik, Universität Hannover, Herrenhäuserstraße 2, 30419 Hannover, Germany; †Department of Molecular Biology, Glaxo Institute for Molecular Biology, Chemin des Aulx 14, 1228 Geneva, Switzerland; and ‡Max-Delbrück-Laboratorium in der Max-Planck-Gesellschaft, Carl von Linne Weg 10, 50829 Köln, Germany

Communicated by Winslow R. Briggs, Carnegie Institution of Washington, Stanford, CA, December 26, 1995

ABSTRACT **KAT1 is a voltage-dependent inward rectifying K^+ channel cloned from the higher plant *Arabidopsis thaliana* [Anderson, J. A., Huprikar, S. S., Kochian, L. V., Lucas, W. J. & Gaber, R. F. (1992) *Proc. Natl. Acad. Sci. USA* 89, 3736–3740]. It is related to the Shaker superfamily of K^+ channels characterized by six transmembrane spanning domains (S1–S6) and a putative pore-forming region between S5 and S6 (H5). The H5 region between Pro-247 and Pro-271 in KAT1 contains 14 additional amino acids when compared with Shaker [Aldrich, R. W. (1993) *Nature (London)* 362, 107–108]. We studied various point mutations introduced into H5 to determine whether voltage-dependent plant and animal K^+ channels share similar pore structures. Through heterologous expression in *Xenopus* oocytes and voltage-clamp analysis combined with phenotypic analysis involving a potassium transport-defective *Saccharomyces cerevisiae* strain, we investigated the selectivity filter of the mutants and their susceptibility toward inhibition by cesium and calcium ions. With respect to electrophysiological properties, KAT1 mutants segregated into three groups: (*i*) wild-type-like channels, (*ii*) channels modified in selectivity and Cs^+ or Ca^{2+} sensitivity, and (*iii*) a group that was additionally affected in its voltage dependence. Despite the additional 14 amino acids in H5, this motif in KAT1 is also involved in the formation of the ion-conducting pore because amino acid substitutions at Leu-251, Thr-256, Thr-259, and Thr-260 resulted in functional channels with modified ionic selectivity and inhibition. Creation of Ca^{2+} sensitivity and an increased susceptibility to Cs^+ block through mutations within the narrow pore might indicate that both blockers move deeply into the channel. Furthermore, mutations close to the rim of the pore affecting the half-activation potential ($U_{1/2}$) indicate that amino acids within the pore either interact with the voltage sensor or ion permeation feeds back on gating.**

KAT1 was cloned from an *Arabidopsis thaliana* cDNA library by functional complementation of a yeast mutant deficient in K^+ uptake (1, 2). Using the oocyte-expression system, Schachtman *et al.* (3) were the first who demonstrated that KAT1 carries a voltage-dependent inward-rectifying K^+ current. Further studies have shown that KAT1, the "green" inward rectifier, gains its voltage dependence through an intrinsic voltage sensor (4) rather than a block through cytoplasmic Mg^{2+} as shown for its animal counterpart (5). With respect to the gating mechanism, KAT1 is therefore more closely related to the outward-rectifying Shaker-type channels. In common with Shaker, KAT1, a member of the plant inward rectifiers, shares an overall molecular structure of six hydrophobic domains (S1–S6), one of which is positively charged (S4), and an amphiphilic stretch of amino acids (H5) between S5 and S6 (Fig. 1*A*) (7). The latter two motifs are very likely to be part of the voltage sensor (S4) and part of the ion permeation pathway (H5) (8, ¶, ‖). So far, however, chimera between KAT1 and Shaker on one side (9) and eag on the other**, including S4, did not affect inward rectification. Therefore, other membrane domains as well as intra- or extracellular sites may contribute to the voltage-sensing mechanism.†† ‡‡

Whereas different laboratories found an increase in macroscopic current through the green K^+ channel at hyperpolarized membrane potentials (3, 4, 10–12), conflicting single channel conductances have been reported. Hedrich *et al.* (4) and Hoshi (12) could show that a single 5-pS rather than a 34 pS (3, 13, 14) channel generated the inward currents following the expression of KAT1 in *Xenopus* oocytes.

A KAT1-related K^+ channel, KST1, cloned from an epidermal fragment library of potato (*Solanum tuberosum*), is expressed in guard cells and flowers (15). KST1 is characterized by a voltage- and ATP-dependent 7-pS K^+ channel when functionally expressed in oocytes. An apparently plant-specific feature of KAT1 and KST1 is their activation by acidic pH (refs. 4, 10, 12, and 15; cf. ref. 16). pH activation is achieved by a shift in the half-activation potential ($U_{1/2}$) toward less negative or even positive potentials (refs. 4 and 12; for lack of modulation of the voltage sensor, see ref. 10). In addition to the Shaker-related features of KAT1, a putative ATP- and cyclic nucleotide-binding domain was deduced from the primary structure of this plant K^+ channel (17). In line with the postulated role of these structural motifs, activation of KAT1 and KST1 by ATP and cGMP has been demonstrated (12, 15).

Herein we show that mutations in H5 alter the Rb^+ permeability, the susceptability to block by Cs^+ and Ca^{2+}, as well as voltage sensitivity of the green Shaker channel.

MATERIALS AND METHODS

Generation of KAT1 Mutants. KAT1 mutants were generated by polymerase chain reaction (PCR) as described by H.A. Erlich (18). The mutations were introduced into the 3′ oligonucleotide used for PCR amplification. The PCR was performed using AmpliTaq polymerase (Perkin–Elmer/Cetus) on an Applied Biosystems PCR machine. The amplified PCR

The publication costs of this article were defrayed in part by page charge payment. This article must therefore be hereby marked "*advertisement*" in accordance with 18 U.S.C. §1734 solely to indicate this fact.

Abbreviation: TEA, tetraethylammonium.

§To whom reprint requests should be addressed.

¶Becker, D., Dreyer, I., Palme, K. & Hedrich, R. (1995) 10th International Workshop on Plant Membrane Biology, Regensburg, abstr. C51.

‖Chilcott, T. C., Frost-Schartzer, S., Iverson, M. W., Garvin, D., Kochian, L. V. & Lucas, W. J. (1995) 10th International Workshop on Plant Membrane Biology, Regensburg, abstr. C54.

**Hoshi, T., Marten, I. & Henneger, D. J. (1995) 10th International Workshop on Plant Membrane Biology, Regensburg, abstr. L15.

††Bosseux, C., Daram, P., Lemaillet, G., Sentenac, H. & Thibaud, J. B. (1995) 10th International Workshop on Plant Membrane Biology, Regensburg, abstr. C53.

‡‡Lemaillet, G., Ros, R. & Sentenac, H. (1995) 10th International Workshop on Plant Membrane Biology, Regensburg, abstr. C61.

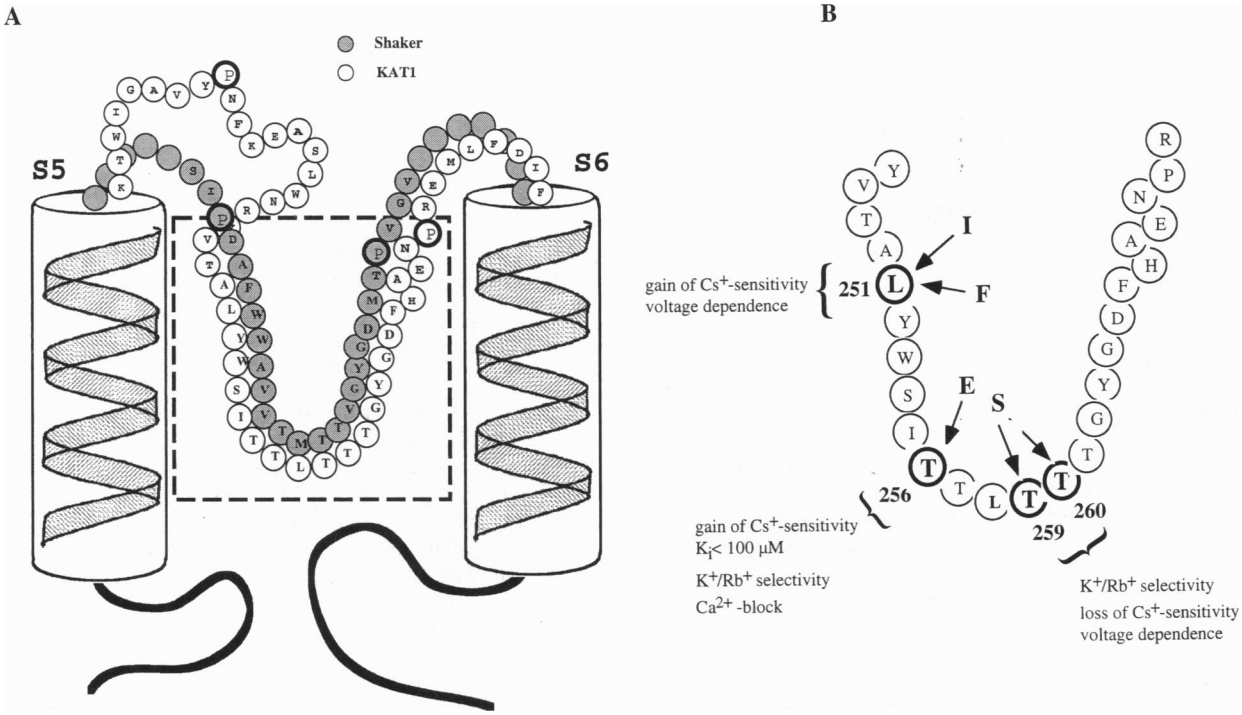

FIG. 1. Diagram of the putative pore of KAT1 and Shaker. (*A*) Residues forming the loop between predicted transmembrane segments 5 and 6. The stretch of amino acids between the marked Pro residues have been shown to line the narrow pore in Shaker (6). In KAT1, 14 additional amino acids were found between Pro-247 and Pro-271, the supposed bounds for the entry and exit of the plant pore region. (*B*) Leu-251, Thr-256, Thr-259, and Thr-260, the four residues that were mutated within this study, are indicated by arrows.

fragments were subcloned into pUC19 and sequenced. The mutated fragments were inserted into the KAT1 cDNA as a *Bsp*HI fragment and the reconstituted mutant cDNA was cloned into the pGEMHE expression cassette (19).

Yeast Genetics. The construction of the *Saccharomyces cerevisiae* strain used in this study: JRY339, *MATa trk1::ura3Δ456*, *trk2Δ1::hisG*, *ura3Δ*, is described in Lichtenberg-Frate *et al.* (20). Yeast strains were maintained on SDAP medium (21) containing 2% purified agar (Sigma A-7921) supplemented with KCl. KAT1 and mutants were subcloned in the expression vector pPGK (22) containing the 3-phosphoglycerate kinase promoter and terminator. Yeast transformations were performed using the lithium acetate method (23).

Injection of cRNA in *Xenopus* Oocytes. *Xenopus* frogs were purchased from Nasco (Fort Atkinson, WI). Oocytes were isolated as described by Stühmer *et al.* (24) and injected with cRNA (100 ng/μl) using a General Valve Picospritzer II microinjector [40 psi (1 psi = 6.89 kPa) for 5–10 ms].

Voltage-Clamp Recordings. Whole-cell K^+ currents were measured with a two-microelectrode voltage-clamp (Turbotec 01C, NPI Germany), by using 0.5- to 2-MΩ pipettes filled with 3 M KCl as described (15). Since Véry *et al.* (10) described that some channel properties of KAT1 differ with the expression rate, we selected for further analysis oocytes with similar KAT1 expression.

Single-Channel Recordings (Patch-Clamp). Data acquisition and single-channel experiments were performed as described (4, 15). The bath solution contained 100 mM potassium gluconate, 2 mM $MgCl_2$, 2 mM EGTA, 10 mM Tris/Mes (pH 7.4), and 1 mM MgATP. Patch pipettes were loaded with 100 mM potassium gluconate/2 mM $MgCl_2$/1 mM $CaCl_2$/10 mM Mes/Tris (pH 5.6). The osmolality in both media was balanced with D-sorbitol to 220 milliosmoles.

Solutions. Solutions for selectivity experiments contained 2 mM $MgCl_2$, 1 mM $CaCl_2$, 10 mM Mes/Tris (pH 5.6), 100 mM KCl, 100 mM RbCl, 100 mM NH_4Cl, 100 mM LiCl, and 100 mM NaCl, respectively. Solutions for Cs^+ experiments contained 30 mM KCl, 2 mM $MgCl_2$, 1 mM $CaCl_2$, 10 mM Mes/Tris (pH 5.6), and 10 μM to 10 mM CsCl. Solutions for Ca^{2+} experiments on the mutant T256E contained 30 mM KCl, 2 mM $MgCl_2$, 10 mM Mes/Tris (pH 5.6), and various mole fractions at 30 mM of $CaCl_2$ and $MgCl_2$ used to maintain the ionic strength. All solutions were adjusted to 220 milliosmolal with sorbitol.

Data Analyses. *Selectivity.* Relative permeability for Rb^+ and NH_4^+ was calculated according to

$$\frac{P_X}{P_K} = \frac{[K^+]}{[X^+]} \exp\left[\left(\frac{F}{RT}\right)\cdot\Delta U_{rev}\right]$$

from the shift in reversal potential ($\Delta U_{rev.}$) after replacement of 100 mM KCl with RbCl or NH_4Cl in the bath.

Cs^+ sensitivity. Current–voltage relationships of tail currents were fitted according to Woodhull model (25):

$$I(U) = I_0(U)\left\{\frac{1}{1 + \exp\left[-(zF/RT)\delta(U - U_{Block1/2})\right]}\right\},$$

where $I_0(U)$ denotes the current in the absence of Cs^+. The half-blocking voltage $U_{Block1/2}$ could be obtained from $I(U_{Block1/2}) = \frac{1}{2} \times I_0(U_{Block1/2})$.

Table 1. Characteristics of pore mutants of KAT1

	Relative permeability			$K_i(Cs^+)$,		Shift in
	K^+	Rb^+	NH_4^+	μM	$\delta_{Cs+block}$	$U_{1/2}$
KAT1 WT	100	34 ± 2	5 ± 1	335 ± 93	1.6 ± 0.3	–
T199S	100	29 ± 3	5 ± 1	312 ± 120	1.5 ± 0.1	–
L251I	100	34 ± 5	6 ± 2	112 ± 43	1.4 ± 0.3	+
L251F	100	41 ± 5	5 ± 1	212 ± 43	1.3 ± 0.1	–
T256E	100	64 ± 9	9 ± 1	20 ± 2	—	–
T259S	100	48 ± 5	6 ± 1	1110 ± 238	1.7 ± 0.2	–
T260S	100	80 ± 18	7 ± 1	1703 ± 302	0.8 ± 0.2	+
T259/260S	100	49 ± 4	6 ± 1	622 ± 129	1.3 ± 0.2	+

Susceptability toward block by Cs^+ ions in 30 mM KCl is given by the inhibition constant K_i at −180 mV. The electrical distance $\delta_{Cs+Block}$ in 30 mM KCl was determined according to Woodhull (25). Data represent the mean ± SD of three to nine measurements.

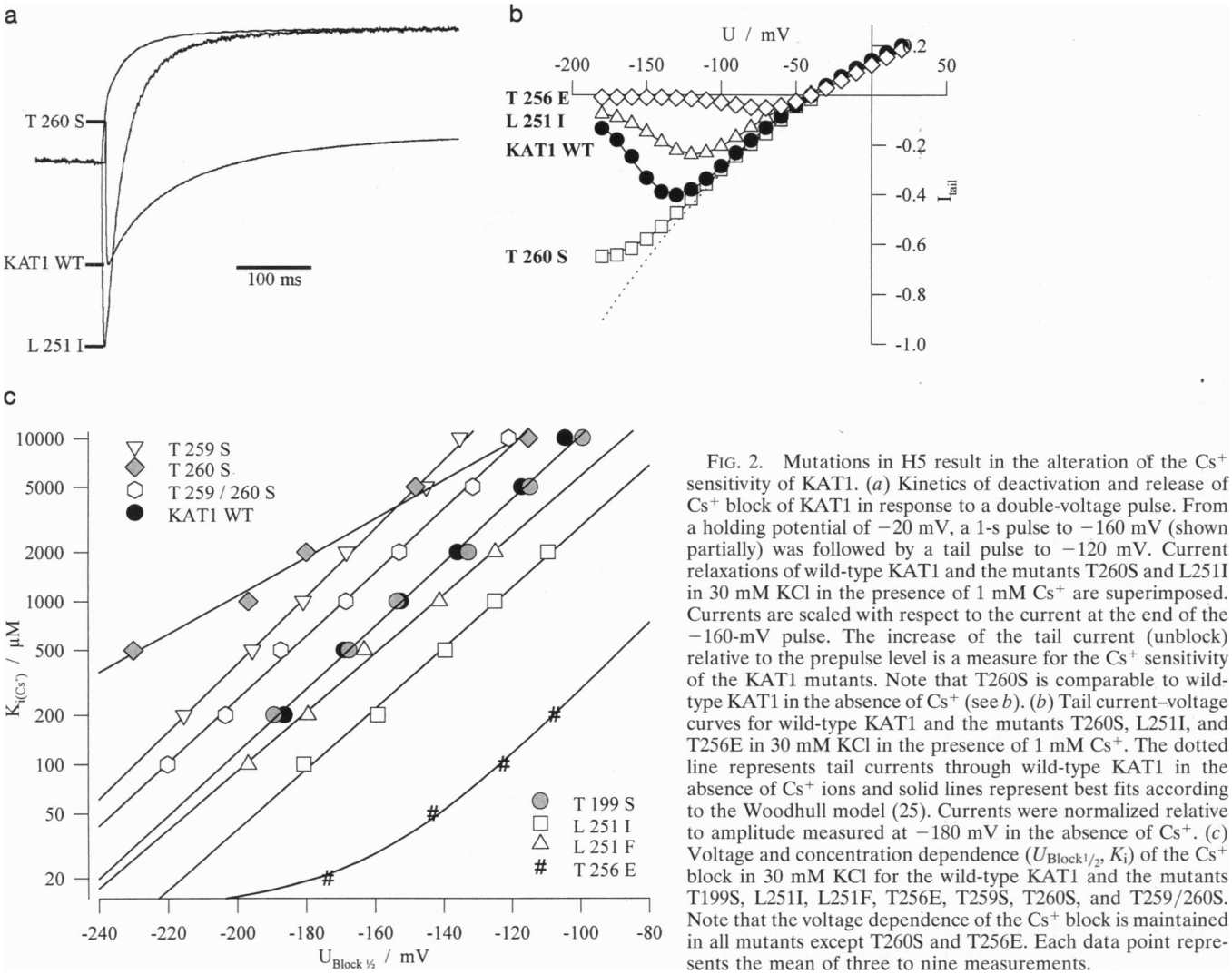

FIG. 2. Mutations in H5 result in the alteration of the Cs^+ sensitivity of KAT1. (*a*) Kinetics of deactivation and release of Cs^+ block of KAT1 in response to a double-voltage pulse. From a holding potential of −20 mV, a 1-s pulse to −160 mV (shown partially) was followed by a tail pulse to −120 mV. Current relaxations of wild-type KAT1 and the mutants T260S and L251I in 30 mM KCl in the presence of 1 mM Cs^+ are superimposed. Currents are scaled with respect to the current at the end of the −160-mV pulse. The increase of the tail current (unblock) relative to the prepulse level is a measure for the Cs^+ sensitivity of the KAT1 mutants. Note that T260S is comparable to wild-type KAT1 in the absence of Cs^+ (see *b*). (*b*) Tail current–voltage curves for wild-type KAT1 and the mutants T260S, L251I, and T256E in 30 mM KCl in the presence of 1 mM Cs^+. The dotted line represents tail currents through wild-type KAT1 in the absence of Cs^+ ions and solid lines represent best fits according to the Woodhull model (25). Currents were normalized relative to amplitude measured at −180 mV in the absence of Cs^+. (*c*) Voltage and concentration dependence ($U_{Block1/2}$, K_i) of the Cs^+ block in 30 mM KCl for the wild-type KAT1 and the mutants T199S, L251I, L251F, T256E, T259S, T260S, and T259/260S. Note that the voltage dependence of the Cs^+ block is maintained in all mutants except T260S and T256E. Each data point represents the mean of three to nine measurements.

RESULTS AND DISCUSSION

Selectivity. Most inward rectifiers in plant cells studied so far, including the gene products of *Kat1* and *Kst1*, are permeable to K^+ and Rb^+ but often impermeable to Na^+ and Li^+ (13). A corn coleoptile K^+ channel, however, is an exception in that its Rb^+ permeability is strongly reduced (26). In addition, both the plant inward rectifiers, which have been

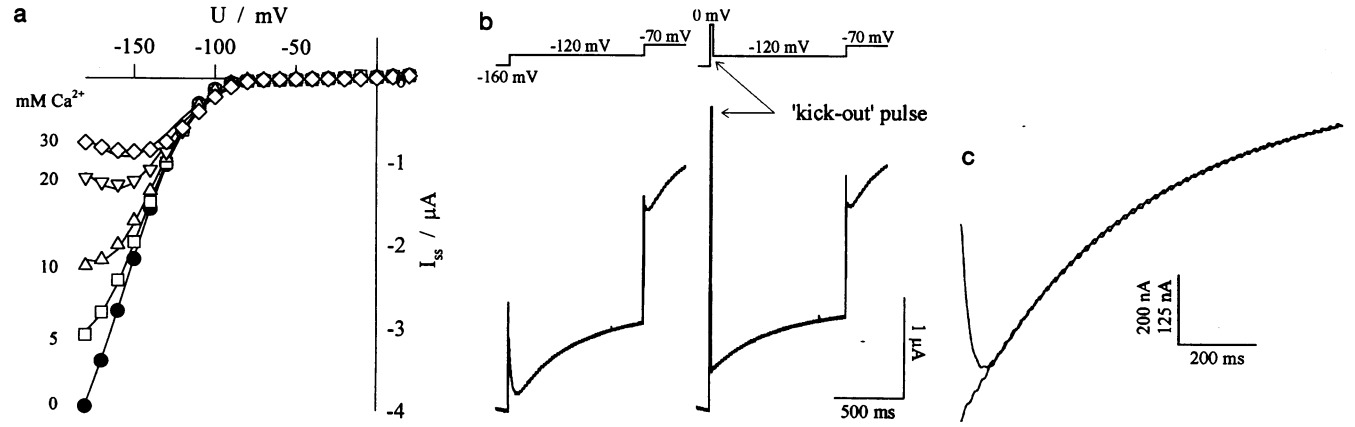

FIG. 3. Calcium ions block inward K^+ currents of the KAT1 mutant T256E. (*a*) Steady-state current–voltage relationship in the presence of Ca^{2+} in the external solution. Since Mg^{2+} did not block the inward currents, the ionic strength was balanced with $MgCl_2$. Solid lines represent best fits according to the Woodhull model (25). (*b*) The Ca^{2+} unblock kinetics of T256E resolved by tail experiments. After an activating prepulse to $U = -160$ mV for $t = 1$ s (shown partially) in the following tail pulse to $U = -120$ mV unblock and deactivation kinetics superimpose (left trace). The unblock kinetics is completely eliminated by an initial short depolarizing step (10 ms) to 0 mV (kick-out pulse). The deactivation process procedes as in the absence of Ca^{2+} (right trace). (*c*) During the intermediate depolarizing pulse, not only were the blocking ions removed from the pore but also some channels were deactivated according to $I(t) = I_0 \times \exp(-t/\tau)$, with $\tau \approx 20$ ms (12). Since the amplitude of the current was thus smaller by a factor of $\exp(-10\text{ ms}/20\text{ ms}) \approx 0.6$ than without the deactivating prepulse, the superposition shows the normal and the scaled tail after a kick-out pulse.

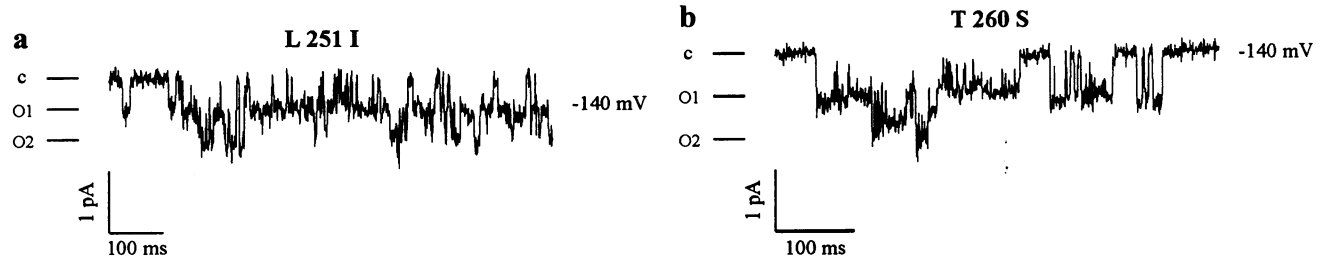

FIG. 4. The most diverse Cs^+-sensitive mutants L251I and T260S are not affected in their single-channel conductance when compared with wild-type KAT1. Inside-out patches were excised from *Xenopus* oocytes expressing the H5 mutants T260S and L251I of KAT1. o, Open channel; c, closed channel.

studied in their natural environment, as well as the gene products of *Kat1* and *Kst1* analyzed in *Xenopus* oocytes, are characterized by a high NH_4^+ conductance (3, 4, 15, 26). We therefore generated channel mutants in H5 and analyzed them with respect to their permeability for Rb^+ and NH_4^+.

Inward K^+ current through these mutated channels showed the slow activation kinetics charactistic of the wild-type channel (3, 4), when elicited by hyperpolarizing voltage pulses. None of the introduced replacements significantly affected the relative NH_4^+ permeability $P_{NH4}+/P_K+$. Although a ratio of 0.06 ± 0.01 in wild type and mutants (Table 1) indicated that the selectivity filter favors K^+ transport, the half-saturation constants for both ions, $K_m(K^+)$ = 39 mM (in line with previous findings, ref. 27) and $K_m(NH_4^+)$ = 47 mM, however, were rather similar.

Since Thr-441 in Shaker is part of the selectivity filter (28), we mutated the corresponding amino acid Thr-259 in KAT1 to Ser (Fig. 1). The T259S mutation as well as the mutation of Thr-260 to Ser (T260S) altered the relative Rb^+ permeability ($P_{Rb}+/P_K+$) from 0.34 in the wild-type channel to 0.48 and 0.80 in the mutants. The simultaneous mutation of both Thr-259 and Thr-260 to Ser resulted in a relative permeability ratio for $P_{Rb}+/P_K+$ of 0.49, indicating that in the double mutant T259S is dominant (for inverse behavior with respect to shifts in the activation curve, see Fig. 5 and corresponding text below).

Susceptability to Blocking Cations. In contrast to their animal counterparts, which subdivide into two classes according to their tetraethylammonium (TEA^+) sensitivity (<1 mM and >20 mM; refs. 29 and 30), all plant K^+ channels studied have exhibited a low affinity for external TEA^+ ($K_i \approx$ 10–30 mM), the cationic K^+ channel blocker. This behavior is possibly due to the lack of corresponding high-affinity amino acids in H5 (31, 32) including Thr-449 and Asp-431 in Shaker or Tyr-380 in Kv2.1 (6) compared with Thr-249 and His-267 in KAT1 (Fig. 1). Plant growth and K^+ channel activity, however, are extremely sensitive to Cs^+ (4, 10, 15, 26, 33), which in contrast to TEA^+ causes voltage-dependent blockade (4, 10). To elucidate whether the change in Cs^+ sensitivity correlates with the location of the mutated amino acid relative to the transmembrane electrical field, we measured the relative voltage drop sensed by the Cs^+ according to the Woodhull model (25). The block of KAT1 by Cs^+ is strongly voltage-dependent, increasing its strength with increasing negative voltages (Fig. 2*b*). An electrical distance δ of >1 was calculated (Table 1). Therefore, for KAT1, like the inward rectifier in the starfish egg (34, 35), a multi-ion single-file pore has to be assumed to describe permeation through the K^+ channel and the observed features of the interaction with Cs^+ (36). A supposed competition of both ions for at least two common binding sites was additionally supported by the finding that δ changed with the external K^+ concentration (data not shown).

The various point mutations in H5 could be distinguished by their differences in Cs^+ sensitivity up to a hundredfold (Table 1). When we replaced Thr-259 or Thr-260 with Ser (T259S or T260S), the K_i for Cs^+ at −180 mV increased by a factor of 3 or 5, respectively, compared with wild type. Interestingly, the double mutant T259/260S is more sensitive to Cs^+ than any of the two single mutants. (Fig. 2 *a* and *b* and Table 1). In addition to residues Thr-259 and Thr-260, which were presumed to contribute to the selectivity filter, we mutated Leu-251 in KAT1, because at this position there is an Ile in a corn coleoptile and broad bean leaf channel, and a Phe in Shaker (unpublished results). In contrast to the conserved exchanges at positions 259 and 260, mutations L251I and L251F resulted in an increase in Cs^+ sensitivity (Table 1). In Fig. 2*a*, the response of wild-type KAT1, L251I, and T260S to a double voltage pulse is superimposed. In the presence of 1 mM Cs^+, K currents through these channels slowly activate during a 1-s prepulse to −160 mV. Upon the subsequent step to −120 mV, the tail current decreased toward a new steady state in T260S (zero current level in the case of T260S and L251I, but not wild type, see Fig. 5). In contrast, KAT1 wild-type and L251I tails initially increased (Fig. 2*a*). This increase in current has previously been demonstrated to result from unblock of Cs^+ from the open channel (4, 15, 26). Thus, T260S in the presence of 1 mM Cs^+ responded almost like the wild-type KAT1 in the absence of the inhibitor (data not shown). In contrast to the reduced Cs^+ sensitivity and voltage dependence of the Cs^+ block in the mutant T260S channel, other exchanges altered the Cs^+ sensitivity while leaving the voltage dependence unaffected (Fig. 2 *b* and *c*). As a control for nonspecific effects of mutagenesis in this experiment, a change of Thr-199 to Ser, outside the

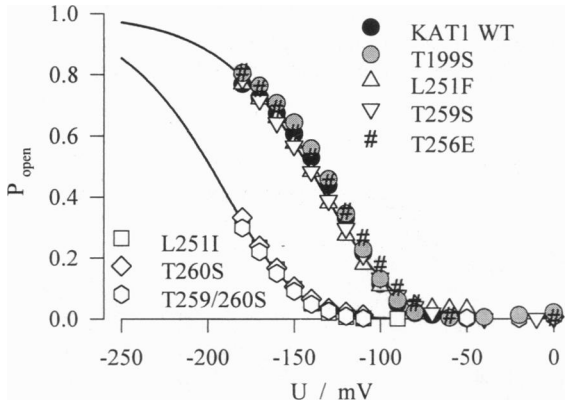

FIG. 5. Mutations within H5 shift the voltage-dependent open probability of KAT1. The mutants L251I and T260S and the double mutant T259/260S but not T199S, L251F, T256E, and T259S are characterized by an half-activtion potential ($U_{1/2}$) shifted by about 60 mV more negative than wild-type KAT1. The determination of the half-activation potentials was based on activation-curve analyses as described (4). When plotting the ratio between the steady-state currents and the corresponding tails as a function of voltage, a measure for the voltage-dependent open probability, P_{open}, of single KAT1 channels, best fits for wild-type and mutant channels were obtained when a cooperativity of four identical channel subunits (S4 segments) was assumed, an approach described for potassium channels (12). The solid lines represent the best fits according to $P_0 = \{1/[1 + \exp(ZF/RT)(U - U_{1/2})]\}^n$, with z = 1.3 and n = 4.

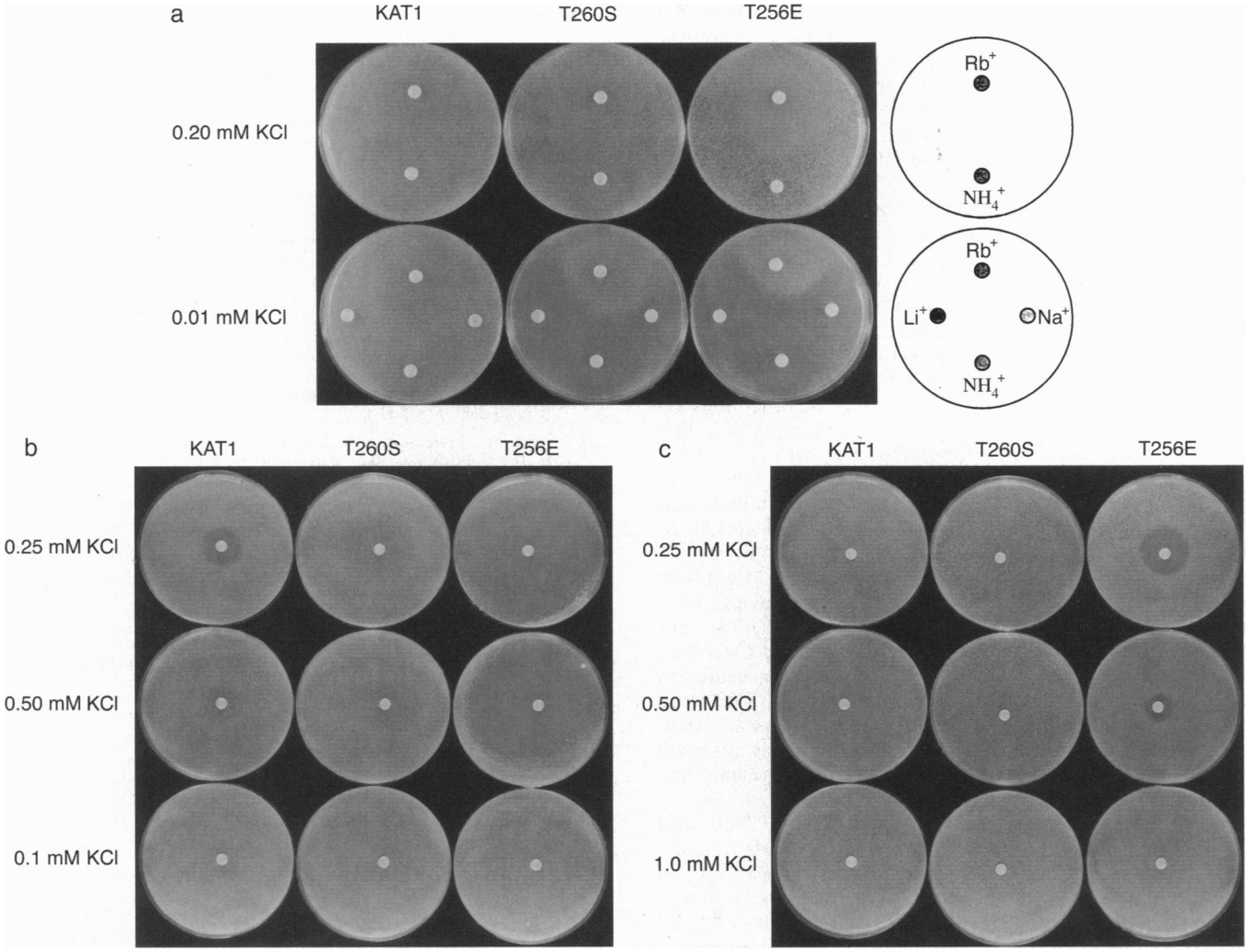

FIG. 6. Selectivity and blockade of wild-type KAT1, T260S, and T256E mutant channels *in vivo*. The effect of monovalent and divalent cations on growth was detected by the halo assay. A lawn of 10^5 cells of JRY339 expressing KAT1, T260S, or T256E was plated in 1% agar on SDAP plates supplemented with the indicated concentration of KCl. A paper disk containing 10 μl of the test cation solution was placed on the agar surface and the plates were incubated at 30°C for 36 h. In the growth zone around the disk, inhibition creates a dark halo whereas stimulation creates a reverse halo. Concentration and position of each test solution: (*a*) RbCl (1 M), upper disk; NH_4Cl (1 M), lower disk; LiCl (10 M), left disk, lower row; NaCl (5 M), right disk, bottom row. (*b*) CsCl (1 M). (*c*) $CaCl_2$ (1 M).

putative pore region, exhibited properties indistinguishable from wild-type KAT1 (Fig. 2*c* and Table 1; see Fig. 5).

In contrast to the guard-cell K^+ uptake channels from *Vicia faba*, *Zea mays* (37, 38), *Solanum tuberosum*, and *Nicotina tabaccum* (unpublished results), KAT1 is not blocked by external Ca^{2+} up to 30 mM. We therefore introduced a charged amino acid at position 256, corresponding to Val-438 in Shaker, which is supposed to interact with the GYG and thus to line the narrow pore. Replacing Thr with Glu, T256E, drastically altered the permeation properties of the channel. Whereas the selectivity sequence was within the range described for the other mutants (Table 1), the sensitivity toward Cs^+ increased by a factor of 15 compared with the wild type and up to 100 compared with T260S. Even more interesting, this mutant developed a Ca^{2+} sensitivity similar in voltage and concentration dependence to that described for the inward rectifying K^+ channel in guard cells of *Vicia faba* (Fig. 3) (37, 38). In Fig. 3, the blocking Ca^{2+} is released by a depolarizing voltage pulse to -120 mV. In contrast to the Cs^+ block, the voltage-dependent interaction of the calcium with the open pore could be described with a δ of 0.5, indicating that a single Ca^{2+} might move 50% of the voltage drop (25). The unblock could be described by a single exponential. The deactivation in the absence of Ca^{2+} and after unblock was identical (Fig. 3*c*).

Single-Channel Conductance and Voltage Dependence. Patch-clamp studies revealed that the single-channel conductances of the most diverse and conservative amino acid exchanges containing Cs^+-sensitive mutants L251I and T260S of 5 ± 1 pS ($n = 3$) and 7 ± 2 pS ($n = 2$) were comparable with 5–6 pS for wild-type KAT1 and 7 pS for KST1 (Fig. 4) (4, 12, 15). When we compared the voltage dependence of the H5 mutants, however, two groups could be identified: L251F and T259S had half-activation potentials ($U_{1/2}$) comparable to wild type, whereas L251I, T260S, and T259/260S exhibited activation curves shifted by about 60 mV toward more negative voltages (Fig. 5). An apparent gating charge of $z = 1.3$ indicated that the voltage sensitivity of the KAT1 mutants remained unaffected. It should be noted that the double mutant T259S/T260S shifted the activation curve in the same way as T260S (Table 1 and Fig. 5). Hence, in the double mutant the T259S exchange was dominant with respect to ion permeation (see above) while the T260S exchange was dominant with respect to activation-threshold shifts. An analogous mutation to KAT1 T260S in Shaker (T442S) caused a similar shift in the activation threshold (28). Since this effect was not analyzed further, we cannot distinguish between the possibilities that in KAT1, where the shift was even more pronounced, amino acids within the pore either interact with the voltage sensor or the

permeating ion affects its own gating. The complex interaction between the pore-forming domain and the voltage sensor was illustrated by the fact that a conservative exchange at position 251 from Leu to Ile strongly influenced the voltage dependence of activation, whereas the more drastic exchange from Leu to Phe did not affect this parameter. Likewise, the introduction of a negative charge into the narrow pore left the voltage dependence unaffected.

Functional Expression in Yeast. *S. cerevisiae* strain JRY339, in which the *TRK1* and *TRK2* genes (2) have been deleted, does not grow on growth medium containing less than 1 mM KCl; growth can be rescued by expression of KAT1 (1). We tested whether KAT1 with either of two mutations in the H5 region would allow growth in low K^+ medium. The T256E and T260S mutant channels restored the growth of strain JRY339 on medium containing 0.2 mM KCl but unlike KAT1 they did not grow with only 0.01 mM KCl. The effect of other ions on growth was tested by placing an impregnated paper disk on a nascent lawn of yeast cells suspended in growth agar. After incubation for 36 h, growth inhibition was reflected by a clear halo around the disk and growth stimulation by an increased density (reverse halo). RbCl strongly stimulated growth of T256E and T260S, but slightly inhibited growth of the KAT1 strain (Fig. 6*a*). $NHCl_4$ and $MgCl_2$ had no effect. In contrast to KAT1, cells expressing T256E were supersensitive to inhibition by CsCl (Fig. 6*b*) and $CaCl_2$ (Fig. 6*c*). The T260S mutant cells were unaffected by $CaCl_2$ and less sensitive to CsCl than either T256E or KAT1 (Fig. 6*b*); however, when measured at 24 h, there was clear inhibition by CsCl. NaCl and LiCl were strongly inhibitory to T260S cells, but only weakly inhibitory to T256E and KAT1. Whenever growth inhibition was observed (for KAT1 and both mutants), the diameter of the halo was larger at lower potassium concentrations.

These results demonstrate that both KAT1T256E and KAT1T260S express functional K^+ uptake channels in yeast. Growth on low K^+ was strongly affected by certain cations and was different for each mutant. Despite the qualitative nature of the growth assay, the diameter of the reverse halos produced by Rb^+ stimulation was in line with the PK/PRb permeability ratios of the mutant channels (Table 1), and the degree of inhibition by Cs^+ or Ca^{2+} correlated with data obtained from voltage-clamp recordings of whole cell K^+ currents (Figs. 2 and 3). Therefore, the phenotype conferred by each mutation most likely resulted from the direct action of specific cations on ion-uptake through the mutant channels. Thus, the removal of a methyl group from the sidechain of a conserved Thr in the signature sequence allowed Rb^+ to permeate the T260S channel and thereby activate intracellular processes that are required for growth. The substitution of an acidic Glu residue at T256 resulted in increased permeation by Rb^+ and a dramatic increase in inhibition by Cs^+ and Ca^{2+}. The finding that the degree of inhibition by Cs^+ and Ca^{2+} changed with the external KCl concentration, suggests a competition between K^+ ions and blocking cations for residues in the P region that are exposed to the aqueous lumen of the pore.

We are grateful to Chris Readhead (Köln) for helpful comments on the manuscript. Furthermore, we thank Alan North (Geneva), Mohamed El Alama, and Kerstin Neuwinger for expert technical assistance and Angelika Küch and Birgit Reintanz for support in the generation of H5 mutants. This work was funded by Deutsche Forschungsgemeinschaft grants to R.H. (1640/1–3) and R.H. and K.P. (1640/9–10).

1. Anderson, J. A., Huprikar, S. S., Kochian, L. V., Lucas, W. J. & Gaber, R. F. (1992) *Proc. Natl. Acad. Sci. USA* **89,** 3736–3740.
2. Ko, C. H. & Gaber, R. F. (1991) *Mol. Cell. Biol.* **11,** 4266–4273.
3. Schachtman, D. P., Schroeder, J. I., Lucas, W. J., Anderson, J. A. & Gaber, R. F. (1992) *Science* **258,** 1654–1658.
4. Hedrich, R., Moran, O., Conti, F., Busch, H., Becker, D., Gambale, F., Dreyer, I., Küch, A., Neuwinger, K. & Palme, K. (1995) *Eur. Biophys. J.* **24,** 107–115.
5. Kubo, Y., Baldwin, T. J., Jan, Y. N. & Jan, L. Y. (1993) *Nature (London)* **362,** 127–132.
6. Brown, A. M. (1993) *Annu. Rev. Biophys. Biomol. Struct.* **22,** 173–198.
7. Aldrich, R. W. (1993) *Nature (London)* **362,** 107–108.
8. Uozumi, N., Gassmann, W., Cao, Y. & Schroeder, J. I. (1995) *J. Biol. Chem.* **270,** 24276–24281.
9. Cao, Y., Crawford, N. M. & Schroeder, J. I. (1995) *J. Biol. Chem.* **270,** 17697–17701.
10. Véry, A. A., Gaymard, F., Bosseux, C., Sentenac, H. & Thibaud, J. B. (1995) *Plant J.* **7,** 321–332.
11. Bertl, A., Anderson, J. A., Slayman, C. L., Sentenac, H. & Gaber, R. F. (1995) *Proc. Natl. Acad. Sci. USA* **92,** 2701–2705.
12. Hoshi, T. (1995) *J. Gen. Physiol.* **105,** 309–328.
13. Hedrich, R. & Becker, D. (1994) *Plant Mol. Biol.* **26,** 1637–1649.
14. Methfessel, C., Witzemann, V., Takahashi, T., Mishima, M., Numa, S. & Sakmann, B. (1986) *Pflügers Arch.* **407,** 577–588.
15. Müller-Röber, B., Ellenberg, J., Provart, N., Willmitzer, L., Busch, H., Becker, D., Dietrich, P., Hoth, S. & Hedrich, R. (1995) *EMBO J.* **14,** 2409–2416.
16. Blatt, M. R. (1992) *J. Gen. Physiol.* **99,** 615–644.
17. Schroeder, J. I., Ward, J. M. & Gassmann, W. (1994) *Annu. Rev. Biophys. Biomol. Struct.* **23,** 441–471.
18. Erlich, H. A. (1989) *PCR Technology: Principles and Applications for DNA Amplification* (Stockton, New York).
19. Liman, E. R., Tytgat, J. & Hess. P. (1992) *Neuron* **9,** 861–871.
20. Lichtenberg-Frate, H., Reid, J. D., Heyer, M. & Höfer, M. (1996) *J. Membr. Biol.*, in press.
21. Rodriguez-Navarro, A. & Ramos, J. (1984) *J. Bacteriol.* **159,** 940–945.
22. Kang, Y., Kane, J., Kurjan, J., Stadel, J. M. & Tipper, D. J. (1990) *Mol. Cell. Biol.* **10,** 2582–2590.
23. Geitz, R. D. & Schiestl, R. H. (1991) *Yeast* **7,** 253–263.
24. Stühmer, W., Methfessel, C., Sakmann, B., Noda, M. & Numa, S. (1987) *Eur. Biophys.* **14,** 131–138.
25. Woodhull, A. (1973) *J. Gen. Physiol.* **61,** 687–708.
26. Hedrich, R., Bregante, M., Dreyer, I. & Gambale, F. (1995) *Planta* **197,** 193–199.
27. Kochian, L. V., Garvin, D. F., Shaff, J. E., Chilcott, T. C. & Lucas, W. J. (1993) *Plant and Soil* **155/156,** 115–118.
28. Yool, J. A. & Schwarz, T. L. (1991) *Nature (London)* **349,** 700–704.
29. Hille, B. (1967) *J. Gen. Physiol.* **50,** 1287–1302.
30. Heginbotham, L. & MacKinnon, R. (1992) *Neuron* **8,** 483–491.
31. Kavanaugh, M. P., Varnum, M. D., Osborne, P. B., Christie, M. J., Busch, A. E., Adelman, J. P. & North, R. H. (1991) *J. Biol. Chem.* **266,** 7583–7587.
32. Hidalgo, P. & MacKinnon, R. (1995) *Science* **268,** 307–310.
33. Sheahan, J. J., Ribeiro-Neto, L. & Sussman, M. R. (1993) *Plant J.* **3,** 647–656.
34. Hagiwara, S. S., Miyazaki, S. & Rosenthal, N. P. (1976) *J. Gen. Physiol.* **67,** 621–638.
35. Hagiwara, S. S., Miyazaki, S., Krasne, S. & Ciani, S. (1977) *J. Gen. Physiol.* **70,** 269–281.
36. Hille, B. & Schwarz, W. (1978) *J. Gen. Physiol.* **72,** 409–442.
37. Busch, H., Hedrich, R. & Raschke, K. (1990) *Plant Physiol.* **93,** 96A.
38. Fairley-Grenot, K. A. & Assmann, S. M. (1992) *J. Membr. Biol.* **128,** 103–113.
39. Lü, Q. & Miller, C. (1995) *Science* **268,** 304–307.